Soft Matter

COMMUNICATION

View Article Online
View Journal | View Issue

Cite this: *Soft Matter*, 2016, 12, 6507

Received 25th May 2016,
Accepted 15th July 2016

DOI: 10.1039/c6sm01203e

www.rsc.org/softmatter

The formation and control of highly crumpled metal surfaces on a photocurable viscous liquid†

Jung Gun Bae,[a] Seung Hyun Sung,[a] Hyemin Lee,[b] Kookheon Char,*[a] Hyunsik Yoon*[b] and Won Bo Lee*[a]

Folds, highly deformed structures, have received extensive attention for their nonlinear responses due to a large strain on soft matters. To investigate the folding phenomena, here, we exploit residual tensile stress during metal deposition, which is large enough to compress a thin film coating and introduce a photocurable viscous fluid to decrease the resistance of the substrate against compressive stress. The system has the advantages of the abilities for freezing the highly deformed surfaces by post-UV exposure to the UV-crosslinkable substrate and manipulating the substrate effect by controlling the thickness of the substrate. We theoretically investigated the dependence on the substrate thickness using scaling analysis and demonstrated self-generated ladder and flower-like graphoepitaxial structures originated from the thickness design of the viscous substrate.

Highly deformed structures exhibit unique behaviours, such as folding, delamination, or cracking, that are relevant to nonlinear responses.[1–5] In particular, folding that exceeds the large deformation limit of buckling has been extensively analysed.[6–9] Folding phenomena resembling wrinkles exist universally in nature over diverse scales, ranging from human lungs to geological stratum.[10–13] There are also systems of folding within wrinkles, such as the leaves of plants.[14] Currently, the high aspect ratio features of wrinkles in soft matter capped with a hard skin bilayer system are attracting extensive attention because they tend to exhibit special functions, such as light trapping in energy harvesting devices or super-hydrophobicity.[15–20] Basically, a large strain applied to a thin film is a requisite for folding.[21] When we alter the substrate to a softer one, we can obtain a folded structure more easily. From this perspective, introducing a fluid substrate instead of the elastomeric solid substrates used in traditional buckling/folding studies is an excellent choice.[22,23] One issue with this approach, however, is that there is a difficulty in maintaining the morphology of thin films. In previous studies, the folding of an elastic film on a viscous liquid layer vanished and turned to a flat state again after stress relaxation.[24]

Here, we present a strategy to form highly crumpled surfaces by exploiting the compressive stress of metal layers during thermal deposition on a liquid prepolymer. To overcome the shortcomings of a fluid substrate system, we used a photocurable polymer to fix the buckled metal film by post-UV exposure. The spontaneous deformation of the thin metal film depends on the thickness of the viscous prepolymer and it was theoretically explained using a scaling model. According to this principle, we could manipulate various crumpled surfaces by geometrical restrictions as well as polymer thickness. Furthermore, we demonstrate ladder and flower-like graphoepitaxial structures originated from the thickness design of viscous substrates and present a replication concept to fabricate the self-generated folding/buckling patterns for repeated use.

Fig. 1a shows a schematic illustration of the experimental procedures. First, to control the thickness of the polymer, we spin-coated a photocurable polyurethane acrylate (PUA, 301RM, Minuta Tech) prepolymer onto a transparent substrate, such as a glass or PET film. Next, we loaded the spin-coated sample with a viscous layer into a thermal evaporator and deposited aluminium under high vacuum ($\sim 10^{-6}$ Torr). Comparing the scanning electron microscopic (SEM) images of the metal surfaces deposited onto a liquid prepolymer and a cured polymer in Fig. 1b and c, respectively, folding and large amplitude buckling obviously occur in the case of the fluidic prepolymer because it lowers the stiffness of the substrate. Out-of-plane deformation occurred because of compressive stress caused by the deposited metal film. The compressive stress is due to the oxidation accompanying volume expansion at the surface during the aluminum deposition on the soft polymer substrate.[25,26]

To prove that aluminum oxidation occurs on the liquid polymer, we deposited 5 nm of aluminum on a partially polymer-coated substrate. As shown in Fig. 1d, the liquid prepolymer is dropped only in the central region. The edge of the substrate without the

[a] *School of Chemical and Biological Engineering, Institute of Chemical Processes, Seoul National University, Seoul 08826, Korea. E-mail: wblee@snu.ac.kr, khchar@plaza.snu.ac.kr*

[b] *Department of Chemical and Biomolecular Engineering, Seoul National University of Science & Technology, Seoul 01811, Korea. E-mail: hsyoon@seoultech.ac.kr*

† Electronic supplementary information (ESI) available. See DOI: 10.1039/c6sm01203e

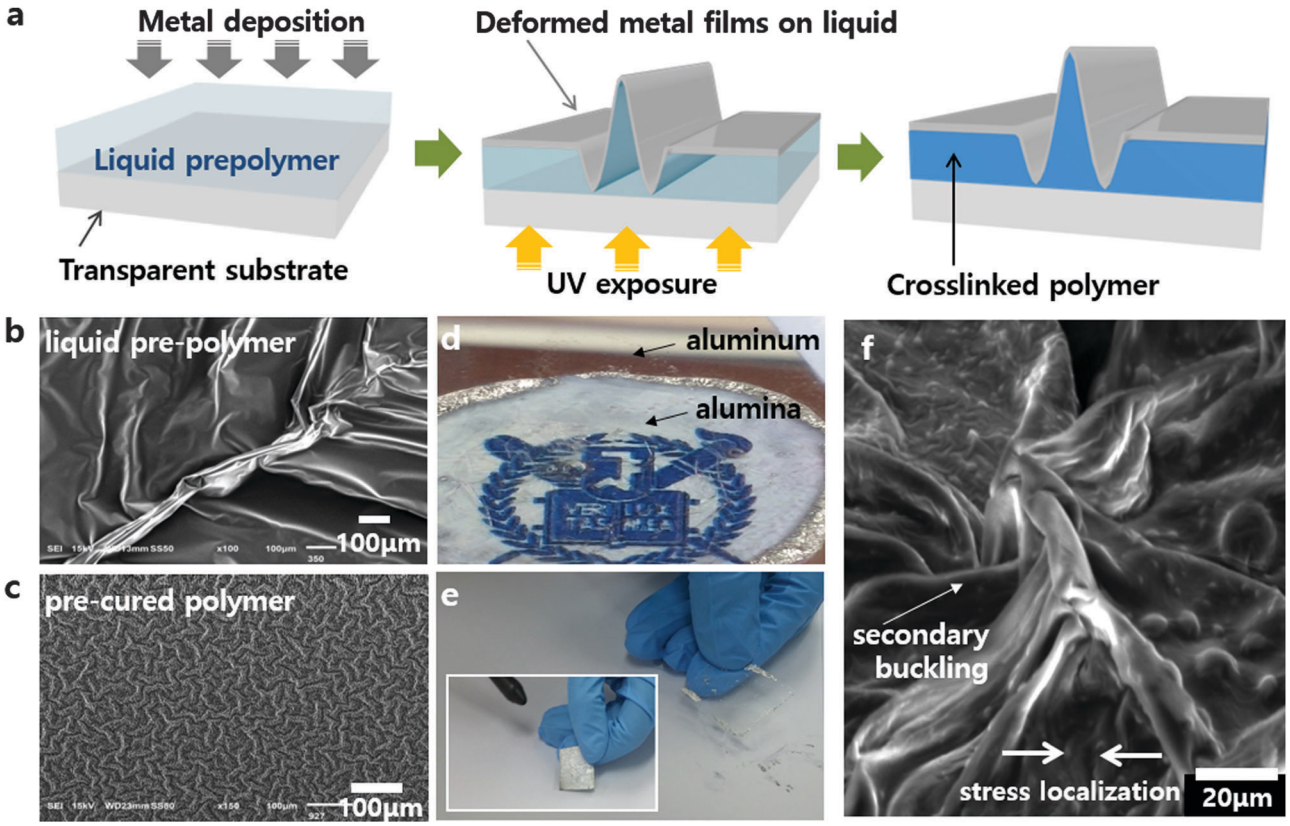

Fig. 1 (a) Schematic illustration of experimental procedures. (b and c) SEM images of buckled surfaces *via* metal deposition (20 nm thick, 0.5 Å s^{-1}) on an un-cured viscous prepolymer and a pre-cured (during 40 s) polymer substrate. (d) Image of the transparent buckled surface resulting from the formation of alumina on a partially coated polymer after 5 nm thick metal deposition. At the edge of the bare glass substrate, aluminum film is deposited directly onto the substrate; a color difference is observed compared to the polymer-coated part. (e) Image of pulverized thin metal film during purging of nitrogen gas without UV exposure after thermal deposition. Inset: See the ESI,† Videos S1 and S2 for a real time movie of a sample with a fully cured polymer substrate that maintained its original shape. (f) A typical SEM image of a high aspect ratio (~1) upward folding. Because of the shallow thickness of the polymer substrate, folding is difficult to develop in the downward direction.

polymer has the metallic color of aluminum. However, the center of the substrate coated with polymer is transparent because Al changes to transparent alumina at the surface of the polymer layer during thermal deposition. As shown in Fig. S1 (ESI†), scanning electron microscopic (SEM) and transmission electron microscopic (TEM) images prove the oxidation of aluminium film during the metal deposition. We note that the direction of stress on the deposited metal films depends on the type of metal.[27] For example, a tensile stress exists when Au film is deposited onto the polymer substrate. Therefore, crack formation occurs during Au deposition on the liquid substrate (see Fig. S2, ESI†).

Deformation of metal is irreversible; thus, the shape of the film is maintained against other cases of fluid substrates (see Fig. S3, ESI†).[24] When pressure is applied on the surface, however, it is pulverized owing to the liquid state of the polymer layer. To freeze the highly deformed surface structure, we expose the bottom of the transparent substrate to UV light as a post-processing step. The fixation of the metal film is verified by purging the surface of the sample with nitrogen gas. On the one hand, when there is no post-exposure, the metal film peels off (Fig. 1e). On the other hand, after post-exposure, the thin metal film is well attached onto the fully cured polymer substrate and maintains its shape. Fig. 1f shows a typical image of upward folding in our system. In addition to the folding, well-ordered secondary buckling is also observed. Under uniaxial compression on a thin film, stress relaxation due to folding causes the other regions of the film to flatten.[1,28] In the case of biaxial compression, the effect of compressive stress, whose direction is perpendicular to that of stress relaxation, is relatively dominant after folding occurs.[29] This phenomenon is the reason why the secondary buckling forms in a perpendicular direction to the folding.

Fig. 2a–c shows 3D confocal microscopic images of the deformed thin metal film on the polymer substrate under the same conditions, but with a varying thickness. The thickness of the polymer is modulated by the control of the spinning speed in the spin-coating process. Interestingly, folding is diminished and finally does not occur as polymer thickness decreases.

To explain the relationship between the folding amplitude and polymer thickness, a simple scaling theory is developed. When the system is under biaxial stress, it can be modelled as a 1D problem based on the assumption that the folding formation mechanism is the same in both directions. The wavelength of buckling λ is determined by competition between

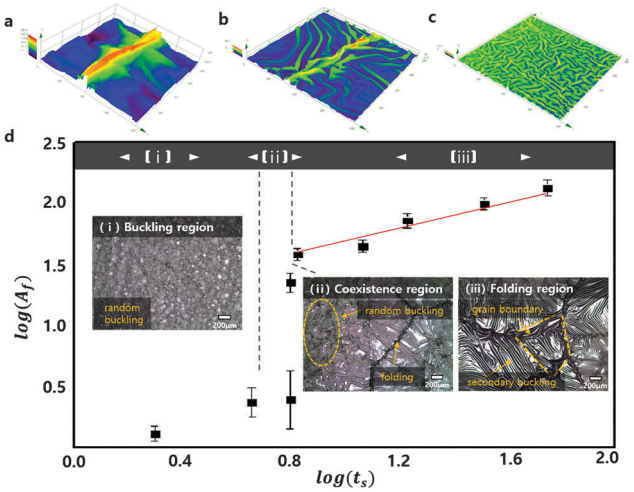

Fig. 2 Three-dimensional images of the deformed surface obtained from confocal microscope data after metal deposition under the same condition, except for the thickness of a viscous layer: (a) 56.6 μm, (b) 6.7 μm and (c) 3.8 μm. The different levels of the undulated surface are represented by color from red (high) to purple (low). (d) Experimental results for the amplitude of folding on different thicknesses of the polymer substrate. A_f is defined as the distance from the highest point of folding to the lowest; however, in the buckling region, it represents the amplitude of buckling. t_s is measured by α-step or cross-sectional SEM imaging. Inner SEM images show the representative parts of the samples.

the stiffnesses of the thin film and the substrate.[10] Therefore, the wavelength is represented by the scaling relation, $\lambda \sim (B/K)^{1/4}$, where B is the bending modulus and K is the effective stiffness of the substrate.[30] According to Cerda and Mahadevan,[30] in the case that the thickness of the substrate t_s is smaller than the characteristic length scale of the bucklings, the stiffness of the substrate is influenced by the thickness of the substrate and is expressed as $K \sim E_s\lambda^2/t_s^3$ where E_s is the Young's modulus of the substrate. Assuming that the time scale of the increase of the compressive stress is much shorter than the relaxation time scale of the viscous polymer, the modulus of the polymer substrate can be approximated to the shear modulus G, which is independent of time. There is also a linear relationship between G and E_s given by $G = E_s/2(1 + \nu)$, where ν is Poisson's ratio.[31]

As a result, the wavelength of the system is given by the following equation:

$$\lambda \sim (E_f/G)^{1/6}(t_f t_s)^{1/2} \quad (1)$$

where E_f and t_f are the Young's modulus and the thickness of the thin metal film, respectively. Because all the experimental parameters except the thickness of substrate are kept constant in our experiments, the wavelength has a scaling relation of $\lambda \sim (t_s)^{1/2}$.

The deformation Δ for folding is proportional to λ from the energy balance approach considered by Pocivavsek *et al.*[1] In addition, the amplitude of folding can be approximated to $\Delta/2$ when the curvature localization is perfect. By using these relations, a final formula related to the amplitude of folding A_f is $A_f \sim (t_s)^{1/2}$. To confirm this scaling relationship, Fig. 2d shows the log–log plot of t_s *vs.* A_f. (A more detailed derivation of the scaling analysis is provided in the ESI† with Fig. S5.) In the folding region, the experimental data are in good agreement with the theoretical line (red), whose slope is 0.5.

Grain boundaries are formed by an overlap of the folds, which have diverse directions. In addition, secondary bucklings are observed in each grain boundary. When the thickness of the prepolymer substrate is thinner than approximately 5 μm, random bucklings cover the surface completely, without folding. These wrinkles are different from well-oriented secondary buckling in the folding region because they are formed in almost random directions. Between those two regions, a coexistence region is found, where folding and random buckling occur simultaneously. We note that the boundary of the folding and the buckling region is where the thickness of the prepolymer is similar to the amplitude of the folding. It is intuitively reasonable that folding is not possible in a thin prepolymer region because the deformed metal surface could attach to the solid substrate and the dissipation of biaxial stress might be slightly relieved by the anchoring effect on both sides of the viscous layer.

To verify the dependence of the substrate thickness on the amplitude of folding, a gradient of polymer thickness is introduced using two different structures. First, an asymmetric ratchet structure filled with prepolymer is prepared, and then aluminium is deposited onto it to form an Al film. As shown in Fig. 3a, a folding bias to the right side of the pattern occurs because the fold develops at the thick region parallel to the hypotenuse of the ratchets (Fig. 3b). When we coated the viscous liquid using the doctor blading method, the pattern trend was not changed (Fig. S4, ESI†).

As shown in Fig. 3c, we use a prepolymer coated line pattern (20 μm heights) that has a gradient resulting from a surface tension driven meniscus. Similarly, folding occurs only at the thick prepolymer region along the wall and secondary bucklings are formed vertical to the folding. To compare three selected locations of secondary buckling from α to γ, their representative

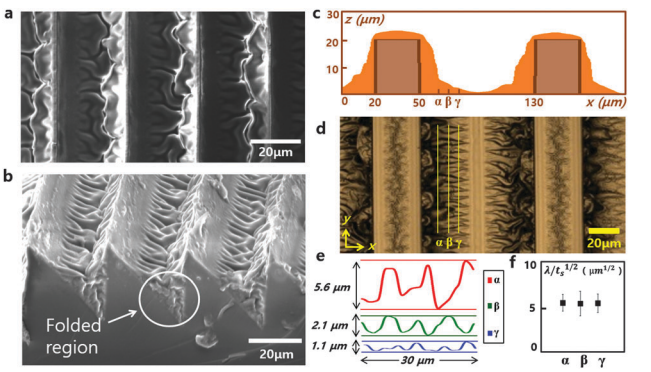

Fig. 3 Planar (a) and cross-sectional (b) SEM images of the deformed surface during the deposition of metal films onto a viscous liquid confined by an asymmetric ratchet array whose period and depth are both 30 μm. (c) Gradient of liquid polymer after spincoating on a microwall pattern, which is obtained by averaging the *x*-directional profile from a confocal microscope image (d). (e) Representative profile of secondary bucklings at locations α to γ. (f) Evaluated value of $\lambda/t_s^{1/2}$ at locations α to γ from the experimental results.

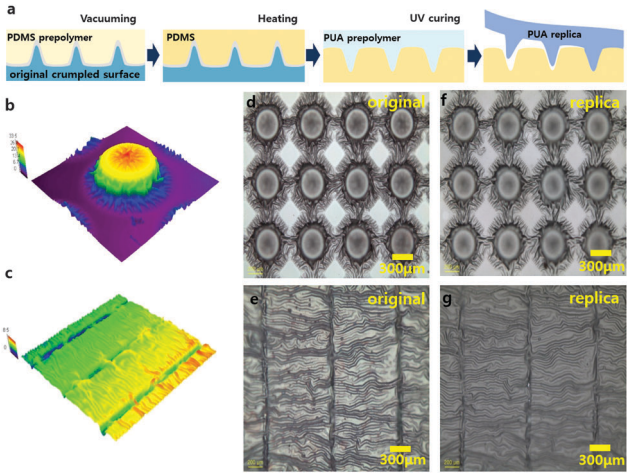

Fig. 4 (a) Schematic illustration of the procedure for obtaining homogeneous polymeric crumpled surfaces using soft lithography. 3D confocal images of the buckled and folded surface on a pillar (b) and a line pattern (c). (d–g) Comparing replicas obtained by soft lithography of the original crumpled surface using optical microscope images of both patterns.

profiles are plotted in Fig. 3e. Their wavelength and amplitude are found to decrease as x increases. Moreover, the measured values of $\lambda t_s^{-1/2}$ in the satellite buckled regions with three different thicknesses (α, β, γ) are nearly constant, which is consistent with the scaling results; thus, the scaling law is relevant to folding as well as buckling.

To repeatedly fabricate structures formed by the combination of folding and wrinkling, we exploited a replication method based on a soft lithographic technique (Fig. 4a). After preparing the deformed surfaces by metal deposition, we poured a polydimethylsiloxane (PDMS) prepolymer mixed with a crosslinker on them. After thermal curing, we detached the PDMS mold from the original wrinkled sample, then we replicated with other polymeric materials such as polyurethane acrylate (PUA) with the mold.

When we deposited aluminium onto a prepolymer surrounding 20 μm heights of a pillar array, satellite bucklings radiated from the center of each pillar. This flower-like surface can be obtained over a large area, as shown in Fig. 4b and d. On a line pattern that is very narrowly carved, folding occurs selectively along the furrow line (Fig. 4c). This result shows that we can manipulate the locations of the folds by exploiting the effect of the differences in substrate thickness. In addition, secondary bucklings that bridge each adjacent folding in a parallel fashion are observed. After the fabrication of the beautifully crumpled surfaces, we replicated the surfaces by soft lithography. As shown in Fig. 4f and g, the replicated surfaces almost perfectly matched the original surfaces.

In conclusion, we proposed a strategy involving aluminium deposition onto photocurable prepolymers to easily form highly deformed surfaces as well as to fix the crumpled surfaces by post-UV exposure. To manipulate the folding and wrinkling, we controlled the thickness of the liquid prepolymer and used confinements prepared using conventional lithographic techniques or mechanical machining. Using scaling theory, we predicted the amplitudes of the folded and buckled regions in terms of the prepolymer thickness. Furthermore, we presented a soft lithographic method to repeatedly fabricate and replicate the beautiful structures formed by the crumpled surfaces.

Acknowledgements

This work was supported by the National Research Foundation of Korea (NRF) grant funded by the Korean government (MSIP) (2013R1A2A2A04015981, 2015R1A2A2A01007379) and by the National Creative Research Initiative Center for Intelligent Hybrids (2010-0018290) through the National Research Foundation of Korea (NRF) grants.

References

1 L. Pocivavsek, R. Dellsy, A. Kern, S. Johnson, B. Lin, K. Y. C. Lee and E. Cerda, *Science*, 2008, **320**, 912–916.
2 F. Brau, H. Vandeparre, A. Sabbah, C. Poulard, A. Boudaoud and P. Damman, *Nat. Phys.*, 2011, **7**, 56–60.
3 G. Wu, Y. Xia and S. Yang, *Soft Matter*, 2014, **10**, 1392–1399.
4 D. Vella, J. Bico, A. Boudaoud, B. Roman and P. M. Reis, *Proc. Natl. Acad. Sci. U. S. A.*, 2009, **106**, 10901–10906.
5 R. L. Kranz, *International Journal of Rock Mechanics and Mining Sciences & Geomechanics Abstracts*, Elsevier, 1979, vol. 16, pp. 37–47.
6 H. Diamant and T. A. Witten, *Phys. Rev. Lett.*, 2011, **107**, 164302.
7 F. Brau, P. Damman, H. Diamant and T. A. Witten, *Soft Matter*, 2013, **9**, 8177–8186.
8 B. Audoly, *Phys. Rev. E: Stat., Nonlinear, Soft Matter Phys.*, 2011, **84**, 11605.
9 D. P. Holmes and A. J. Crosby, *Phys. Rev. Lett.*, 2010, **105**, 38303.
10 J. Genzer and J. Groenewold, *Soft Matter*, 2006, **2**, 310–323.
11 J. A. Zasadzinski, J. Ding, H. E. Warriner, F. Bringezu and A. J. Waring, *Curr. Opin. Colloid Interface Sci.*, 2001, **6**, 506–513.
12 N. J. Price and J. W. Cosgrove, *Analysis of geological structures*, Cambridge University Press, 1990.
13 E. Cerda, *J. Biomech.*, 2005, **38**, 1598–1603.
14 Y. Couder, L. Pauchard, C. Allain, M. Adda-Bedia and S. Douady, *Eur. Phys. J. B*, 2002, **28**, 135–138.
15 Y. C. Chen and A. J. Crosby, *Adv. Mater.*, 2014, **26**, 5626–5631.
16 J. Zang, S. Ryu, N. Pugno, Q. Wang, Q. Tu, M. J. Buehler and X. Zhao, *Nat. Mater.*, 2013, **12**, 321–325.
17 D.-Y. Khang, H. Jiang, Y. Huang and J. A. Rogers, *Science*, 2006, **311**, 208–212.
18 J. A. Rogers, T. Someya and Y. Huang, *Science*, 2010, **327**, 1603–1607.
19 E. P. Chan, E. J. Smith, R. C. Hayward and A. J. Crosby, *Adv. Mater.*, 2008, **20**, 711.
20 J. Kim, J. Yoon and R. C. Hayward, *Nat. Mater.*, 2010, **9**, 159–164.
21 Y. Ebata, A. B. Croll and A. J. Crosby, *Soft Matter*, 2012, **8**, 9086–9091.

22 H. Diamant and T. A. Witten, *Phys. Rev. E: Stat., Nonlinear, Soft Matter Phys.*, 2013, **88**, 12401.
23 J. Huang, M. Juszkiewicz, W. H. De Jeu, E. Cerda, T. Emrick, N. Menon and T. P. Russell, *Science*, 2007, **317**, 650–653.
24 S. Chatterjee, C. McDonald, J. Niu, S. S. Velankar, P. Wang and R. Huang, *Soft Matter*, 2015, **11**, 1814–1827.
25 H. Yoon, A. Ghosh, J. Y. Han, S. H. Sung, W. B. Lee and K. Char, *Adv. Funct. Mater.*, 2012, **22**, 3723–3728.
26 Z. Suo, *J. Mech. Phys. Solids*, 1995, **43**, 829–846.
27 H. Yoon, H. Woo, M. K. Choi, K. Y. Suh and K. Char, *Langmuir*, 2010, **26**, 9198–9201.
28 P. M. Reis, F. Corson, A. Boudaoud and B. Roman, *Phys. Rev. Lett.*, 2009, **103**, 45501.
29 P. Kim, M. Abkarian and H. A. Stone, *Nat. Mater.*, 2011, **10**, 952–957.
30 E. Cerda and L. Mahadevan, *Phys. Rev. Lett.*, 2003, **90**, 74302.
31 J. Gere and B. Goodno, *Mechanics of materials*, Nelson Education, 2012.